Book ISBN: 978-952-412-288-7 | Series ISSN 2709-7609 (Online) | License: CC BY-NC-ND 4.0 | Pages: 10

FACILITY COMMISSIONING FOR EXPERIMENTS ON LIQUID-TO-VAPOR EXPANSION OF ORGANIC FLUIDS

Riccardo Gioia[1], Alessandro Romei[1], Andrea Spinelli[1*]

[1] *Politecnico di Milano, Energy Department, via Lambruschini 4, 20156 Milano, Italy*
* Corresponding Author: andrea.spinelli@polimi.it

ABSTRACT

The increasing interest in partial evaporation organic Rankine cycles, which are theoretically more efficient than traditional single-phase cycles in converting low-temperature waste heat into electricity, is encountering challenges in the development of reliable models to describe the flashing process occurring within the expander. These challenges stem from the lack of experimental data relevant to this process. To address this need, the TROVA facility (Test Rig for Organic Vapours) at Politecnico di Milano - a blowdown wind tunnel that has been successfully used to characterize single-phase organic flows - has been modified to investigate the liquid-to-vapor expansion of organic dry fluids through converging-diverging nozzles. The initial phase of the commissioning process is delineated in this paper, with a particular emphasis on the characterization of molecular nitrogen expansion through pressure measurement and schlieren visualization. During the commissioning tests, the proper operation of the modified facility was verified, as well as the experimental data characterizing the nozzle flow, which showed good agreement with the results of CFD simulations. This enabled us to conclude that the initial commissioning of the modified facility was satisfactory.

1. INTRODUCTION

In the last decade, the need to mitigate climate change by decarbonizing primary energy consumption has increased interest in recovering medium- and low-temperature waste heat released by the industrial sector, which accounts for approximately 26% of the EU primary energy demand (Agathokleous *et al.*, 2019). Various technologies have been proposed to efficiently harness these low-carbon energy sources, among which the conversion of waste heat into electricity through an organic Rankine cycle (ORC) - primarily in its single-phase configuration - has received particular attention.

More recently, modifications to the cycle configuration have been proposed to improve efficiency when utilizing low-temperature heat sources. One such approach involves achieving a better match with the heat source temperature profile by selecting the endpoint of the evaporation phase, thereby reducing exergy losses. Based on this concept, partial evaporation cycles (Daniarta *et al.*, 2021) and trilateral flashing cycles (Elliot, 1982) have been introduced. In the partial evaporation cycle, the heating phase concludes within the saturation dome (vapor quality $0 \leq X \leq 1$), whereas in the trilateral cycle, it ends under saturated (or slightly subcooled) liquid conditions ($X \approx 0$). As demonstrated by White (2021), two-phase cycles can achieve a relative efficiency increase of up to 28% compared to equivalent single-phase cycles when operating with heat sources at around 150 °C. However, this advantage is conditional upon the availability of two-phase expanders with efficiencies comparable to those of single-phase machines. In practice, this requirement typically favors the use of volumetric expanders, which limits the achievable power output to below the megawatt scale.

One possible way to overcome this limitation is to design a single-stage two-phase turbine in which the two-phase expansion occurs exclusively in the stator, ensuring dry operation within the rotor and thereby achieving acceptable efficiency and reliability (White, 2022). This can be accomplished by exploiting the dry behavior of molecularly complex fluids, which allow complete vaporization along adiabatic expansions. However, such processes may involve non-equilibrium phenomena, particularly when expansion does not occur near the critical point of the fluid. As a result, thermodynamic equilibrium models may prove inaccurate and experimentally based models are generally preferred, as has already been done, for instance, for water (De Lorenzo *et al.*, 2017). However, this approach is challenged by the limited availability of experimental data for organic fluids, with the notable exception of the experimental campaign conducted by Zhu and Elbel (2018, 2019). Nevertheless, in this campaign, the use of refrigerant R134a - a fluid lacking a dry saturation curve - and an initial expansion temperature significantly below the typical operating range for ORCs, prevents the collected data from being applied to the development of suitable non-equilibrium models.

To address this gap, an experimental campaign has been launched at the TROVA test rig of Politecnico di Milano, within the framework of the POWHER project. The test rig has been specifically modified to investigate the complete vaporization process of a dry organic fluid, namely hexamethyldisiloxane (MM), starting from subcooled liquid conditions, within a temperature range relevant to ORC applications. This is necessary due to the inherent difficulty of extrapolating data to different operating conditions. An example of a dry-to-liquid expansion is shown in Fig. 1. This work presents the commissioning of the modified test rig and the preliminary experimental results obtained during the facility commissioning, performed with nitrogen as the working fluid.

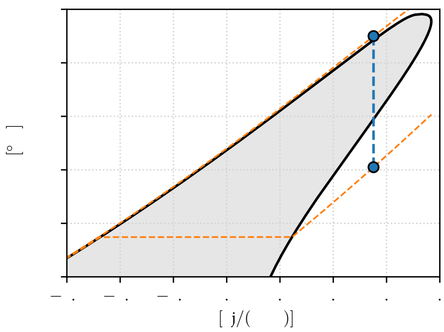

Figure 1: Example of an isentropic liquid-to-dry expansion in the temperature-specific entropy (T, s) diagram for MM. Inlet conditions are $T = 225$ °C and $P = 30$ bar, while outlet pressure is $P = 0.1$ bar.

2. TROVA FACILITY MODIFICATIONS

The TROVA test rig is a blowdown wind tunnel designed to investigate the expansion of organic vapor flows (Spinelli *et al.*, 2013). As illustrated in Fig. 2, the facility consists of a high-pressure vessel (HPV), where the fluid is heated and pressurized through an isochoric process, a test section where the fluid is expanded and characterized, and a low-pressure vessel (LPV), where the fluid is collected and condensed at ambient temperature, thereby ensuring a high-pressure ratio between the two vessels. The experiments previously carried out on the facility were aimed at characterizing non-ideal single-phase flows of organic fluids in saturated/superheated vapor conditions or in a gas-like supercritical state.

The need to characterize wet-to-dry expansions required the construction of a new pipeline to extract subcooled liquid from the HPV, connecting the bottom portion of the vessel to the existing line just upstream of the main control valve (MCV), as shown in Fig. 2. Three ball valves, V5, V6, and V7, have also been installed. Valve V5 isolates the HPV during the heating phase, while V6 and V7 isolate the line not in use (either liquid or vapor operated); for example, V6 is open and V7 is closed when flashing flows are to be investigated, and vice versa for single-phase vapor expansions. A photograph of the new line is provided in Fig. 3a.

A section of the pipeline - heated and insulated with a heating blanket - can be easily replaced with a

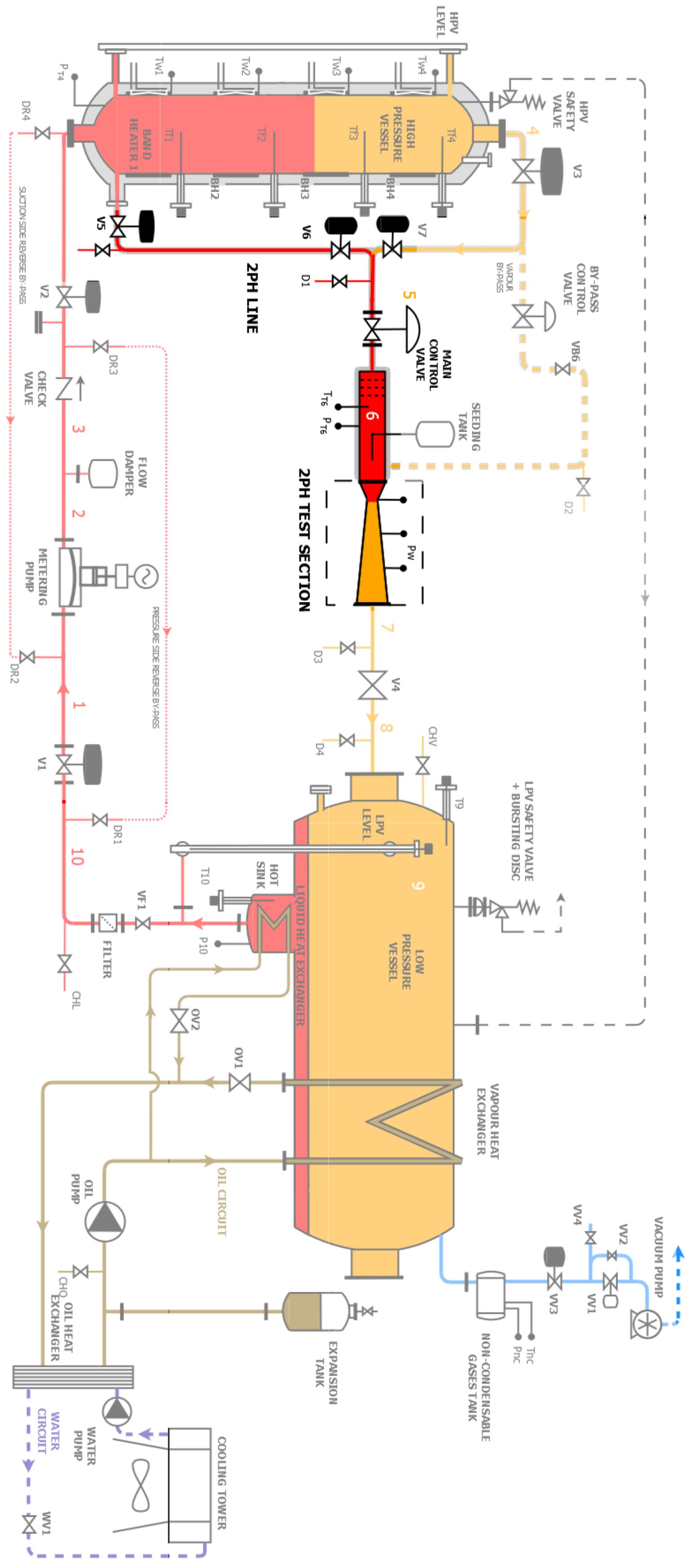

Figure 2: Schematic of the TROVA test rig with the main modifications highlighted.

flow meter, which is currently not installed, to measure the actual mass flow rate in future experiments. This measurement will be used to assess the influence of non-equilibrium effects on the nozzle mass flow rate, in comparison with the value predicted under the equilibrium assumption. In the meantime, optical measurement techniques will be employed to locate the onset of vaporization and detect the appearance of metastable liquid.

A photograph of the test section is shown in Fig. 3b, where the large inlet- and outlet-to-throat area ratio can be appreciated, resulting from the significant density difference between the liquid and vapor phases. The commissioning tests have been conducted using the existing test section (previously employed for single-phase expansions, see for instance Gallarini *et al.* (2021)) equipped with a nozzle profile specifically designed for two-phase experiments. This approach allows the actual feasibility of such tests to be assessed before implementing the dedicated test section (already designed, see Gioia *et al.* (2025)), thus enabling refinements to the final geometry.

The current test section arrangement differs from that designed in Gioia *et al.* (2025) essentially in the location of the pressure taps, the optical measurement technique employed, and the throat area, which in turn affects the test duration. Since the employed test section allows for a shorter admissible nozzle length compared to the one specifically designed for two-phase tests, the nozzle must be scaled by reducing the throat height to approximately 0.75 of the original value, as reported in Tab. 1. However, the scaled throat area is 1.14 times the original one, as the thickness has been increased by approximately 1.52. The effects of this area modification are analyzed in more detail in the following.

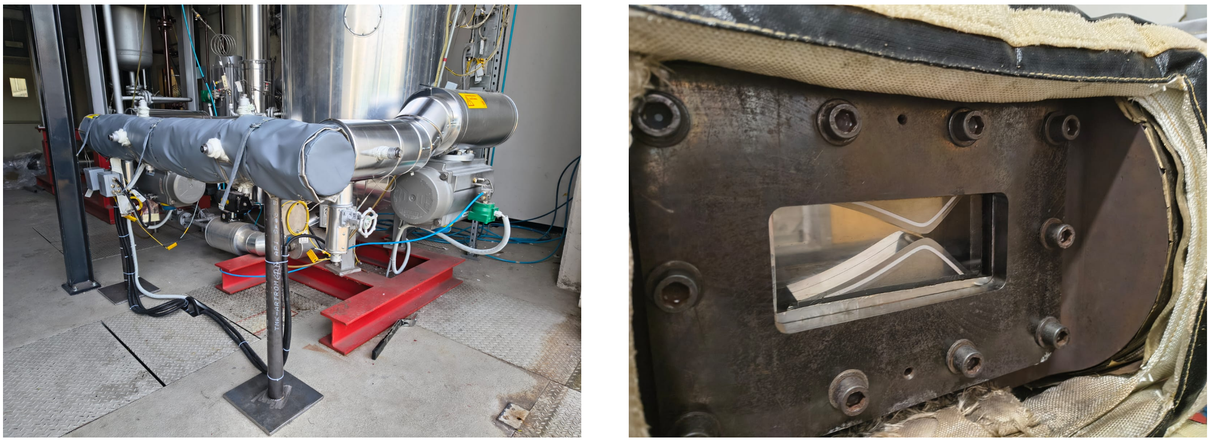

(a) **(b)**

Figure 3: (a) New line and (b) single-phase test section with scaled nozzle pictures. The nozzle flow is from right to left.

The pressure taps are positioned along the nozzle axis rather than along the two profiled walls, which requires one of the planar end walls to be a steel plate with the taps drilled into it. As a result, only a single optical access is available, and the initially planned shadowgraphy technique (which requires optical accesses on both planar end walls) has been replaced with a double-pass schlieren visualization, successfully employed to investigate single-phase expansions (Conti *et al.*, 2017).

Although this technique is not typically used to study two-phase flows, it has been applied in the past with results comparable to those obtained with shadowgraphy (Mauger *et al.*, 2012), since both methods measure changes in the refractive index of the fluid associated with density variations. Nevertheless, particular care must be taken during post-processing, as the inherently opaque nature of two-phase flows (Dash *et al.*, 2018) is expected to produce a dark region downstream of the evaporation onset.

It is worth noting that only expansions beginning from a subcooled or saturated liquid state will be studied. This constraint arises from the current inability to assess both the void fraction and flow regime

Table 1: Main geometrical dimensions of the original and scaled nozzle. The original nozzle has been designed with MM as expanding fluid and with inlet total conditions of $P_{t,in,n} = 19.31$ bar and $T_{t,in,n} = 220.60\,°\mathrm{C}$, while the outlet static pressure is $P_{out,n} = 0.75$ bar.

Nozzle	$y_{in,n}$ **[mm]**	y_{th} **[mm]**	$y_{out,n}$ **[mm]**	L_n **[mm]**	b **[mm]**
Original	96.40	4.10	88.74	188.00	12.30
Scaled	72.00	3.08	66.57	150.41	18.70

upstream of the nozzle, two fundamental parameters necessary for ensuring repeatability and validation.

2.1 Effects of the nozzle change in the test duration

As clarified in the previous section, the use of the single-phase test section required downscaling the originally designed two-phase nozzle profile to allow its installation. Although changes in the flow field are expected to be negligible, the same cannot be said for the test duration, which is limited by the onset of two-phase conditions at the nozzle inlet, since liquid flow must be maintained. The flow rate, governed by the throat area due to the choked nature of the two-phase flow (White, 2022), will increase, resulting in a reduced experiment duration because of the previously described increase in throat passage area.

To predict the useful test duration, a lumped parameter model (Gioia *et al.*, 2025) has been developed to simulate the discharge phase and compute the actual test duration. Figure 4 shows the pressure trend inside the HPV for both the original and scaled nozzles, which have equivalent throat diameters D_{th} of 8 and 8.54 mm, respectively. In both simulations, the fluid is MM, and the initial conditions inside the HPV at $t = 0$ s are $T_{HPV} = 225\,°\mathrm{C}$ and $P_{HPV} = 30$ bar. The time window studied ranges from 0 to 20 s with a discretization of 0.1 s. Note that the choked mass flow rate is obtained by multiplying the equilibrium-based value by a factor of 1.5 to account for the flow rate increase related to the appearance of metastable liquid. A comparison of test durations with the original nozzle, both with and without losses along the upstream line, showed negligible influence of losses on test duration (Gioia *et al.*, 2025); therefore, only inviscid results are reported in Fig. 4. As expected, the time after the opening of the MCV when the pressure at the nozzle inlet approaches the saturation pressure is reduced from 13 to 11.30 s, allowing a useful test duration of about 6.3 s. However, this estimate can increase depending on the decrease in time needed to absorb transient effects associated with the sudden MCV opening, which has been prudently estimated to be around 5 s.

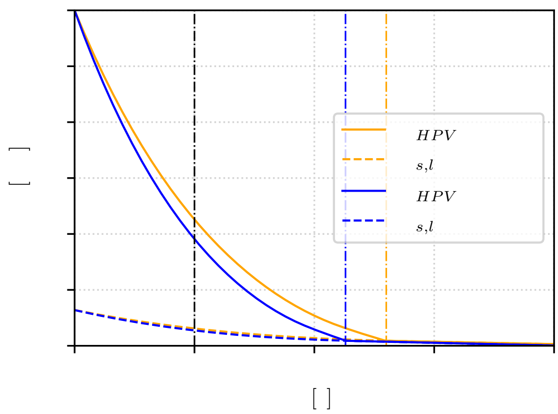

Figure 4: Variation of P_{HPV} and $P_{s,l}$ at the nozzle inlet during the studied time window.

3. EXPERIMENTAL RESULTS AND COMPARISON WITH CFD

This section presents an analysis of the preliminary results obtained from the expansion of molecular nitrogen, along with a comparison between experimental data and CFD simulations.

3.1 Instrumentation, test description and operating conditions

As introduced in Section 2, the main measurement techniques employed during the commissioning phase are pressure and temperature measurements and schlieren visualization.

Regarding pressure measurements, a total of sixteen taps are positioned along the nozzle axis, as shown in Fig. 5, spaced 8.5 mm apart, providing acceptable spatial resolution. The nozzle profile is arranged such that three pressure taps are located in the convergent section, twelve in the divergent section, and one at the geometrical throat. Eleven pressure taps, highlighted in red in Fig. 5, are currently active and connected to locally mounted high-temperature piezoresistive pressure transducers via 40 mm-long pneumatic lines. Total pressure conditions are measured within the plenum using a wall pressure transducer (due to negligible kinetic energy, well below the sensor uncertainty) and two thermocouples of K and J types, with the hot junction positioned at the axis. The expanded uncertainty is below 0.1% of the sensor full scale for pressure and 1 °C for temperature. Data acquisition is performed through analog signal conditioning modules and a high-speed 16-bit ADC board. The acquisition frequency is 1000 Hz, with data averaged in packages of 100 points, resulting in a time resolution of 0.1 s.

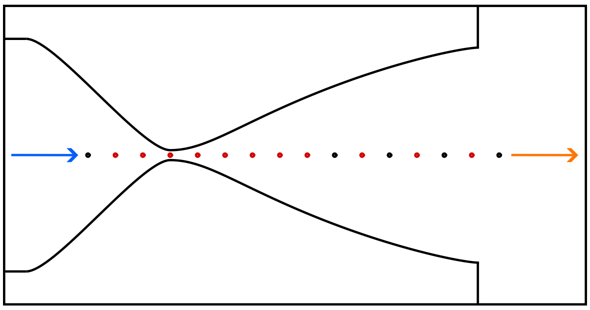

Figure 5: Sketch of the plate mounted in the test section with pressure tap positions and nozzle profile. The pressure taps diameter is not in scale. Red circles indicate active taps, where pressure transducers are mounted.

Regarding schlieren visualization, a double-passage configuration was adopted, allowing the emission and reception components to be mounted on the same optical bench, thus facilitating alignment and enhancing optical sensitivity. This setup requires the backplate, where the pressure taps are drilled, to be mirror-polished. The CMOS camera employed is digitally triggered to synchronize image acquisition with pressure and temperature data. The camera resolution is 1936 x 1216 pixels, with a pixel size of 5.86 µm. The light source is a 1W LED (light-emitting diode) with a dominant wavelength of 460 nm (blue light). Images are acquired at 10 frames per second, with an exposure time of 1 ms.

The discharge of the HPV is initiated by opening the MCV, which remains fully open throughout the entire test duration. Additionally, the blowdown nature of the test rig allows characterization of the expansion in the test section over a wide range of thermodynamic conditions as the HPV empties and the LPV fills, until the two pressures equalize. It is worth noting that the nozzle relaxation time is more than two orders of magnitude shorter than the HPV emptying time (Spinelli *et al.*, 2018). Therefore, the assumption of steady-state flow in the nozzle is valid at any time during the test.

The results reported refer to a single test run starting with total conditions of 12 bar and 15 °C in the HPV, and 0.07 bar in the LPV; this allows exploration of both adapted and over-expanded conditions within a single run.

3.2 CFD framework

Two-dimensional, steady simulations of the nitrogen nozzle flow - corresponding to two different time instants during the commissioning test - are performed using Ansys-Fluent®. The thermodynamic conditions of the process allow the expanded fluid to be modeled as a perfect diatomic gas. The pressure-based coupled solver is employed, with all equations discretized using second-order schemes, while turbulence is modeled using the $\kappa - \omega$ *SST* model, ensuring $y^+ < 5$ along the profile. To reduce computational effort, only half of the passage area of both the nozzle and the downstream plenum is discretized. Smooth-wall boundary conditions are applied at the nozzle and plenum walls. At the inlet, total pressure, total temperature, turbulence intensity, and hydraulic diameter are specified, whereas only static pressure is prescribed at the outlet. Finally, a symmetry boundary condition is imposed along the axis of symmetry. The plenum has been included downstream to ensure a mass-flow averaged Mach number lower than 1 at the domain outlet, thereby enforcing the actual prescribed pressure instead of the adapted one.

Two different simulations were carried out and are described below. The first corresponds to inlet total conditions and outlet pressure measured at 5 s after the MCV opening, while the second uses values measured at 25 s; thus, both adapted and over-expanded flow conditions are simulated. The structured meshes differ between the two simulations: the adapted case ($t = 5$ s) uses approximately $209k$ quadrilateral elements, whereas the over-expanded case ($t = 25$ s) employs around $158k$ cells. While the mesh within the nozzle is identical for both cases, the difference arises from the size of the downstream plenum. To dissipate the majority of kinetic energy before the domain outlet in the adapted condition, a very large plenum is required, with length and height respectively equal to $L_{pl} = 29L_n$ and $y_{pl} = 26y_{out,n}$. For the over-expanded case, where flow separation inside the nozzle reduces the kinetic energy at the outlet, the plenum dimensions are significantly smaller, at $L_{pl} = 0.25L_n$ and $y_{pl} = 1.25y_{out,n}$.

3.3 Experimental results and comparison with the CFD

The comparison of the pressure ratio along the nozzle, shown in Fig. 6a, reveals an almost perfect overlap between the CFD results and the experimental measurements, confirming both the perfect gas assumption and the adapted nature of the flow. This adapted flow condition is further supported by the schlieren image in Fig. 7a, which shows no evidence of shocks or expansion fans. However, this adapted state is short-lived: as the pressure ratio between the HPV and LPV decreases, the nozzle moves to over-expanded conditions. In this regime, shocks begin to appear in the divergent section, inducing flow detachment that propagates upstream as the HPV-to-LPV pressure ratio continues to drop. An example of this flow regime is presented in Fig. 6b, where flow detachment is evident in both the CFD and experimental data, although some differences exist. The CFD profile distinctly captures the shock impact on the axis at $z/L = 0.55$, caused by flow detachment at the nozzle wall, followed by subsequent expansions and weaker shock/expansion waves downstream. Conversely, the experimental pressure ratios exhibit a trend characteristic of a separated subsonic flow. This discrepancy is attributed to the strongly asymmetric and highly unsteady nature of the flow detachment, clearly visible in the schlieren image in Fig. 7b, likely caused by minor asymmetric perturbations in the flow boundary conditions.

It is worth noting that the pronounced flow separation observed here is linked to the markedly different thermodynamic behaviors exhibited during expansion by molecular nitrogen, a simple molecule modeled as an ideal gas, and by flashing MM, a complex molecule undergoing two-phase conditions for which the nozzle was originally designed. In fact, during the actual experimental campaign with MM starting from a subcooled liquid state at the nozzle inlet, little to no flow detachment is expected.

4. CONCLUSIONS

This paper outlines the initial commissioning of the TROVA facility, which was purposefully modified to characterize the liquid-to-dry expansion of an organic dry fluid, specifically hexamethyldisiloxane. The implemented modifications include a new pipeline and a new planar nozzle, while the installation

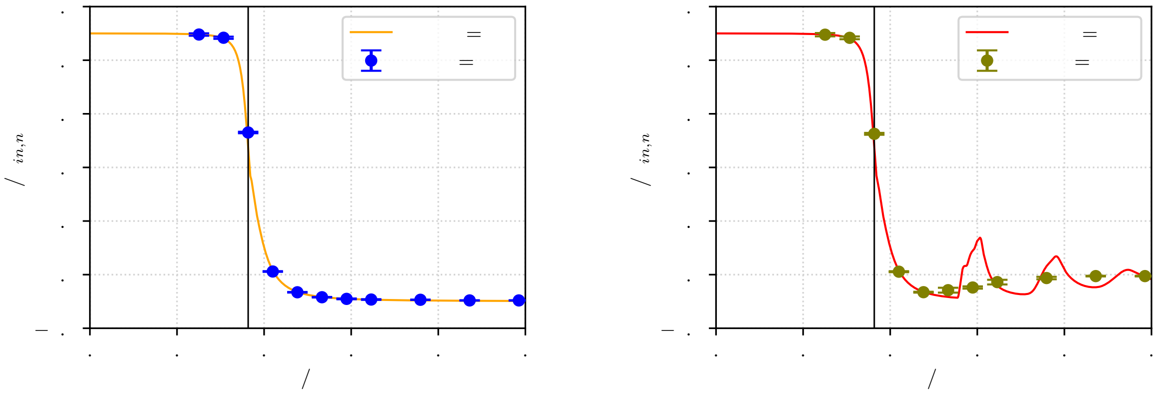

(a) **(b)**

Figure 6: Comparison of the pressure ratio along the nozzle axis between CFD and experimental results (a) at $t = 5\,\text{s}$ and (b) at $t = 25\,\text{s}$. The vertical solid black line locates the geometric throat.

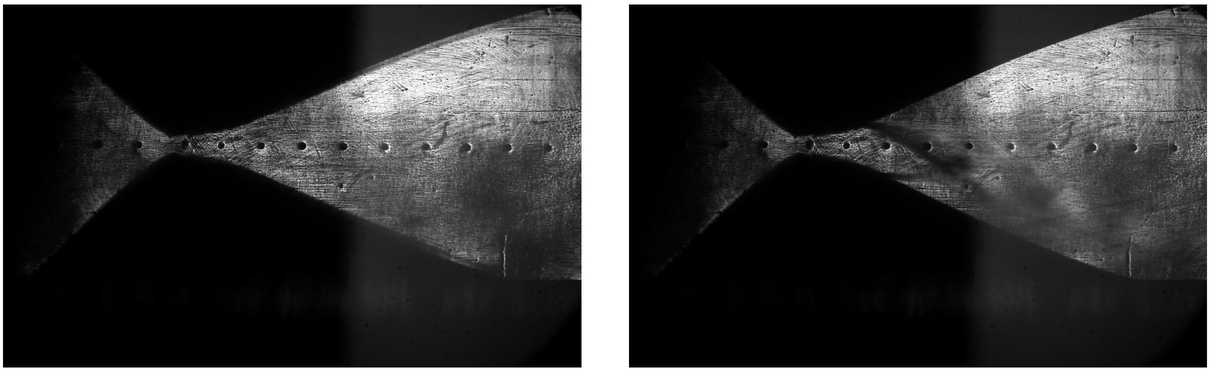

(a) **(b)**

Figure 7: schlieren snapshot (a) at $t = 5\,\text{s}$ and (b) at $t = 25\,\text{s}$.

of a redesigned test section - already completed - is postponed to allow for potential design refinements based on initial experimental results. Additionally, the location of pressure taps was changed from the original experimental design, and the shadowgraphy technique was replaced by schlieren imaging, with only limited expected impacts on two-phase flow characterization.

The results of a commissioning test run using molecular nitrogen as the working fluid are presented through pressure measurements along the converging-diverging nozzle axis and schlieren visualizations at two key time frames representing adapted and over-expanded conditions. Experimental data show good agreement with two corresponding CFD simulations, indicating that the first phase of commissioning has been successful.

Building on these results, the commissioning phase will continue by employing hexamethyldisiloxane vapor to test the heating system and pipe insulation, while also generating more detailed experimental data. The final phase will involve tests with an actual liquid-to-dry expansion, aimed at verifying and, if necessary, improving the measurement techniques and test section design.

NOMENCLATURE

Latin Letters

b	nozzle thickness (mm)
D	equivalent diameter (mm)
L	length (mm)
P	pressure (bar)
$P/P_{in,n}$	pressure ratio
P_t	total pressure (bar)
s	entropy (kj/(kgK))

T	temperature (°C)
t	time (s)
T_t	total temperature (°C)
y	nozzle height (mm)
z/L	non-dimensional axial coordinate

Greek Letters

X	vapor title

Subscripts

$_{HPV}$	high pressure vessel
$_{in,n}$	inlet nozzle
$_{n}$	nozzle
$_{out,n}$	outlet nozzle
$_{pl}$	plenum
$_{s,l}$	saturated liquid
$_{th}$	throat

Abbreviations

CFD	computational fluid dynamic
Exp	experimental
HPV	high pressure vessel
LPV	low pressure vessel
MCV	main control valve
ORC	organic Rankine cycle

REFERENCES

Agathokleous, R., Bianchi, G., Panayiotou, G., Arestia, L., Argyrou, M. C., Georgiou, G. S., Tassou, S. A., Jouhara, H., Kalogirou, S. A., Florides, G. A., and Christodoulides, P. (2019). Waste heat recovery in the eu industry and proposed new technologies. *Energy Procedia*, 161:489–496.

Conti, C. C., Spinelli, A., Cammi, G., Zocca, M., Cozzi, F., Guardone, A., *et al.* (2017). Schlieren visualizations of non-ideal compressible fluid flows. In *13th International Conference on Heat Transfer, Fluid Mechanics and Thermodynamics (HEFAT 2017)*, pages 513–518.

Daniarta, S., Kolasiński, P., and Imre, A. R. (2021). Thermodynamic efficiency of trilateral flash cycle, organic rankine cycle and partially evaporated organic rankine cycle. *Energy Conversion and Management*, 249:114731.

Dash, A., Jahangir, S., and Poelma, C. (2018). Direct comparison of shadowgraphy and x-ray imaging for void fraction determination. *Measurement Science and Technology*, 29:125303.

De Lorenzo, M., Lafon, P., Seynhaeve, J. M., and Bartosiewicz, Y. (2017). Benchmark of delayed equilibrium model (dem) and classic two-phase critical flow models against experimental data. *International Journal of Multiphase Flow*, 92:112–130.

Elliot, D. G. (1982). Theory and tests of two-phase turbines. *Jet Propulsion Laboratory Publication 81-105, Pasadena CA*.

Gallarini, S., Cozzi, F., Spinelli, A., and Guardone, A. (2021). Direct velocity measurements in high-temperature non-ideal vapor flows. *Experiments in Fluids*, 62:199.

Gioia, R., Romei, A., and Spinelli, A. (2025). Design of experiments to observe liquid-to-vapor expansions exploiting molecularly complex organic fluids. In *Proceedings of the 5th International Seminar on Non-Ideal Compressible Fluid Dynamics for Propulsion and Power*. Not published, Springer Nature Switzerland.

Mauger, C., Méès, L., Michard, M., Azouzi, A., and Valette, S. (2012). Shadowgraph, schlieren and interferometry in a 2d cavitating channel flow. *Experiments in Fluids*, 53:1895–1913.

Spinelli, A., Cammi, G., Gallarini, S., Zocca, M., Cozzi, F., Gaetani, P., Dossena, V., and Guardone, A. (2018). Experimental evidence of non-ideal compressible effects in expanding flow of a high molecular complexity vapor. *Experiments in Fluids*, 59:1–16.

Spinelli, A., Pini, M., Dossena, V., Gaetani, P., and Casella, F. (2013). Design, simulation, and construction of a test rig for organic vapors. *Journal of Engineering for Gas Turbines and Power*, 135.

White, M. T. (2021). Cycle and turbine optimisation for an orc operating with two-phase expansion. *Applied Thermal Engineering*, 192:116852.

White, M. T. (2022). Investigating the wet-to-dry expansion of organic fluids for power generation. *International Journal of Heat and Mass Transfer*, 192:122921.

Zhu, J. and Elbel, S. (2018). Experimental investigation of a novel expansion device control mechanism: Vortex control of initially subcooled flashing r134a flow expanded through convergent-divergent nozzles. *International Journal of Refrigeration*, 85:167–183.

Zhu, J. and Elbel, S. (2019). Measurement of static pressure profiles of vortex flashing r134a flow expanded through convergent–divergent nozzles. *International Journal of Refrigeration*, 108:258–270.

ACKNOWLEDGEMENTS

We acknowledge financial support under the National Recovery and Resilience Plan (NRRP), Mission 4, Component 2, Investment 1.1, Call for tender No. 1409 published on 14.9.2022 by the Italian Ministry of University and Research (MUR), funded by the European Union – NextGenerationEU – Project Title: Partial evaporation ORC systems for industrial waste heat recovery - POWHER (P2022MEYKS_002) – CUP D53D23018390001 - Grant Assignment Decree No. 1385 adopted on 01/09/2023 by the Italian Ministry of Ministry of University and Research (MUR).